Pergamon

Deep-Sea Research I, Vol. 41, No. 3, pp. 429–437, 1994

0967–0637/94 $7.00+0.00

Particle trajectories in a rotating cylinder: implications for aggregation incubations

GEORGE A. JACKSON*

(*Received* 8 *February* 1993; *in revised form* 16 *June* 1993; *accepted* 16 *July* 1993)

Abstract—Rotating cylinders offer the possibility of being simple and fast systems to aggregate particles in seawater samples. An analysis of the flow and resulting particle trajectories for such systems under laminar conditions suggests that their dynamics are too complicated for them to be useful for quantitative studies. Among the potential problems are the substantial fluid shear associated with spin up and interactions of particles with container walls.

INTRODUCTION

THE recent interest in marine aggregates has heightened the search for ways to make them in the laboratory. The properties of any device used to incubate water samples should be simple to allow the interpretation of experimental results in terms of aggregation theory.

Aggregation occurs when particles come together and combine. Repeated collision and sticking can form particles much larger than the original source particles. Three physical mechanisms are usually advanced for providing the particle contacts: Brownian motion, shear, and differential sedimentation. Brownian motion is contact resulting from thermal movement of one particle towards the other and is usually insignificant in seawater when both particles are larger than 1 μm (e.g. MCCAVE, 1984). Shear contact occurs when differences in fluid movement carry one particle into another. Such shear can be the result of laminar or turbulent processes. Differential sedimentation occurs when one particle falls faster than the other, overtaking and colliding with it. Rates at which these processes occur depend on the sizes and concentrations of the different particles (e.g. JACKSON, 1989; JACKSON and LOCHMANN, 1992).

The traditional laboratory techniques for coagulating particles have used shear to bring particles together. Using a stirrer to create turbulent shear at a known rate has been a standard tool for sanitary engineers since the work of CAMP and STEIN (1943). It unfortunately creates highly non-uniform turbulent shear, which can destroy aggregates as well as creating them. Using the fluid in a narrow gap between two rotating concentric cylinders rotating can create a known shear field. This system, providing what is known as Couette flow, allows particles denser than the fluid to fall to the bottom when the cylinder axes are vertical.

SHANKS and EDMONDSON (1989) used individual cylinders filled with seawater, rotating on their sides, as their aggregation chambers. A rotating cylinder has the potential to

*Department of Oceanography, Texas A&M University, College Station, TX 77843, U.S.A.

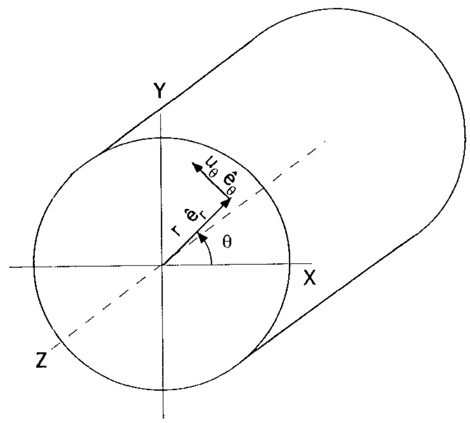

Fig. 1. The coordinate system for the rotating cylinder. Positions and velocities perpendicular to z can be expressed using either the rectangular (x,y) or the cylindrical (r,θ) coordinates.

provide a simple system for studying aggregation in which the dominant mechanism for coagulation is differential sedimentation. However, further use of the rotating cylinder as an experimental aggregation system requires greater understanding of the system properties if it is to provide more than qualitative answers to coagulation questions.

TOOBY *et al.* (1977) analyzed the steady-state motion of a falling particle in such a rotating cylinder. Their analysis showed that particles would follow circular paths if influenced by only the lowest order hydrodynamic effects. An analysis using higher order terms showed that some particles had unstable orbits, following spiral paths either inward or outward. Experimental observations confirmed this.

In this paper, I extend the analysis of cylinder dynamics to include the solution of the flow at startup. The fluid is sheared as the cylinder spins up the interior fluid. Eventually, the shear vanishes as the cylinder and the fluid rotate together in what is known as solid body rotation. I also explore the implications of the fluid motion on particle paths, particularly on particle collisions with the container walls. Such collisions change the particle concentrations and should affect coagulation rates.

MATHEMATICAL TREATMENT

Hydrodynamics

Consider the case of rotating cylinder full of water described using coordinates r, θ and z, where r is the distance from the axis, θ is the angle around the axis and z is the distance along the cylindrical axis (Fig. 1). In these coordinates, the fluid velocity is given by the components (u_r, u_θ, u_z). If the cylinder is long enough and no angle is favored over any other, then the only gradients are in the radial direction and flows in the $\hat{e}_\theta$ direction. The Navier-Stokes equations reduces to

$$\frac{\partial u_\theta}{\partial t} = \nu \left(\frac{\partial^2 u_\theta}{\partial r^2} + \frac{1}{r}\frac{\partial u_\theta}{\partial r} - \frac{u_\theta}{r^2} \right) \tag{1}$$

where ν is the kinematic viscosity (e.g. HAPPEL and BRENNER, 1973).

If the cylinder and all the water contained in it are initially at rest and the container starts to rotate at $t = 0$, then the initial and boundary conditions are

$$u_\theta = \begin{cases} 0 & \text{if } r < a \text{ and } t = 0 \\ \omega a & \text{if } r = a \text{ for } t \geq 0 \end{cases} \tag{2}$$

where a is the radius of the cylinder and ω is the radial velocity of the cylinder.

The solution to this problem is (§7.6, CARSLAW and JAEGER, 1959)

$$u_\theta = \omega r - \sum_{i=1}^{\infty} A_i J_1(\lambda_i r) e^{-\lambda_i^2 \nu t} \tag{3}$$

where $A_i = 2\omega[\lambda_i J_2 \lambda_i a)]^{-1}$ and J_1 and J_2 are Bessel functions of the first kind of orders 1 and 2.

The steady-state solution is solid body rotation, $u_\theta = \omega r$. The remaining terms in equation (3) are harmonics which decay exponentially with time. Values of $\lambda_i a \sim i\pi$ and the decay constants for the higher order terms go as $\lambda_i^2 \sim {}_i^2$. The higher order terms in equation (3) decay away much faster than the lower order ones, with rates proportional to i^2.

The shear rate γ is given by

$$\gamma = r \frac{\mathrm{d}(u_\theta / r)}{\mathrm{d}r}. \tag{4}$$

Differentiation of equation (3) and subsequent simplication yields

$$\gamma = \sum_{i=1}^{\infty} A_i e^{-\lambda_i^2 \nu t} \left[-\frac{\lambda_i}{2} J_0(\lambda_i r) + \frac{1}{r} J_1(\lambda_i r) + \frac{\lambda_i}{2} J_2(\lambda_i r) \right]. \tag{5}$$

The influence of the outer cylinder propagates inward a distance of $\delta \sim (\nu t)^{0.5}$. To reach the center, it would take about 1060 s for $a = 3.25$ cm and about 5600 s for $a = 7.5$ cm. The results can be seen for a system similar to that of SHANKS and EDMONDSON (1989) (Fig. 2b). After 10 s, only a region within about 1 cm of the cylinder wall has started to move. After 100 s, most of the fluid of the fluid in the cylinder has started to move, although there is still a substantial difference between the velocity in the middle and what it will ultimately be. After 1000 s, the cylinder and contained fluid are rotating. Rotation is zero at the center, greatest at the edge. A smaller, more slowly rotating system spins up more rapdily at a rate consistent with the above calculations (Fig. 2a).

Shear is initially very high near the cylinder wall, nonexistent internally (Fig. 3b). After 10 s, the peak shear is 16 s^{-1} about near the edge. After 100 s, the maximum shear is less but shear extends a greater distance into the interior. Although less, it is still 4.6 s^{-1} near the edge and greater than 1 s^{-1} in the outer third of the cylinder, values large compared to typical values for the ocean's interior (e.g. SOLOVIEV *et al.*, 1988). The peak shear is down to 0.28 s^{-1} after 1000 s. The shear has persisted for more than 500 s at a rate of more than 1 s^{-1}. The shear is damped out more rapidly in a smaller cylinder (Fig. 3a). There is no effective shear in it after 1000 s, although there is still shear greater than 0.1 s^{-1} after 100 s.

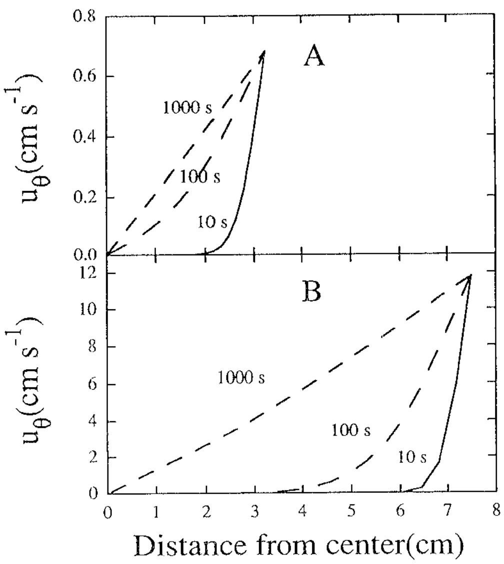

Fig. 2. Fluid velocity as a function of relative distance from the cylinder axis at different times. The values shown are: Case 1 (A) $a = 7.5$ cm, $\omega = 1.57$ s^{-1}, and $\nu = 0.01$ cm^2 s^{-1}; Case 2 (B) $a = 3.25$ cm, $\omega = 0.21$ s^{-1}. Case 1 values typical of the systems used by SHANK and EDMONDSON (1989); Case 2 values typical of more recent systems considered for use (PASSOW and WASSMAN, personal communication). u_θ for steady state (solid body rotation) would be a straight line.

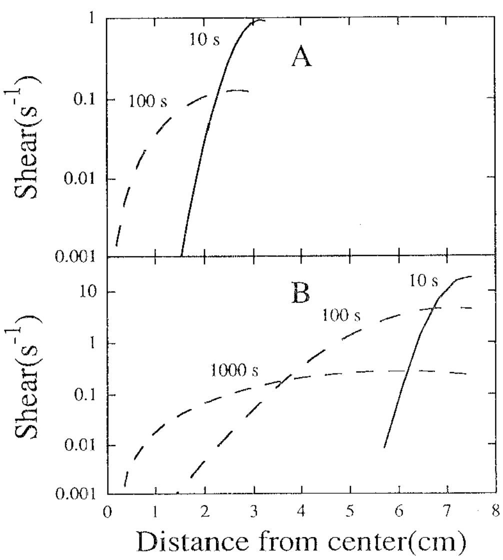

Fig. 3. Fluid shear as a function of relative distance from the cylinder axis for different times. Parameters are the same as those shown in Fig. 2.

Thus, shear can be an important particle collision mechanism during the early parts of a collision experiment and can persist for relatively long periods of time.

Particle trajectories

A particle in the cylinder moves with a velocity that is the sum of its fall velocity and the local fluid velocity. The cylinder is on its side, with gravity perpendicular to its axis in the $-y$ direction. The fluid and the particle move in the xy plane. Changes in particle position are given by

$$\frac{dx}{dt} = -u_\theta \sin\theta$$

$$\frac{dy}{dt} = u_\theta \cos\theta - w_s \tag{6}$$

where w_s is the particle fall velocity and the remaining terms describe the fluid velocity in rectangular coordinates.

For solid body rotation (steady-state motion),

$$x = -r\sin(\omega t - \theta_0) + x_b$$

$$y = +r\cos(\omega t - \theta_0) \tag{7}$$

where θ_0 is the initial particle angle. This set of equations describes circular motion centered around the point $x_b = w_s\omega^{-1}$ on the x axis where a particle's fall velocity would balance the upward fluid velocity.

Equation (7) can be solved numerically for non-steady state conditions when u_θ is known, as is true for the above case of a cylinder initially at rest (equation 3).

The value of w_s can be calculated using any of several formulations. I have used one that has been derived for phytoplankton

$$w_s = 2\xi r_p^{1.17} \tag{8}$$

where r_p is the particle radius and $\xi = 1.24\ \text{cm}^{-0.17}\ \text{s}^{-1}$ (JACKSON, 1989, after SMAYDA, 1970).

The above equations are valid only if the particle does not hit the cylinder wall at $r = a$. Because the particles are assumed to fall downward, they can only intercept the cylinder if $y < 0$. Particles that hit the wall do not bounce because of their small sizes and the small values of Re (e.g. BERG, 1983). Once a particle hits the cylinder wall its velocity cannot have a component perpendicular to the wall but can parallel to it. I allowed particles that hit the wall to move with this parallel component. Particles fall away from the wall once $y > 0$.

PARTICLE TRAJECTORIES

Fluid at steady state

For a fluid at steady state, solid body rotation, particles must be within a distance of $a - x_b$ from the balance point $(x_b, 0)$ if they are to avoid the cylinder wall. Any other

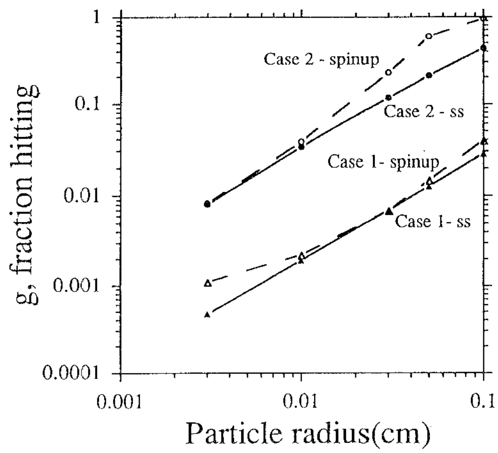

Fig. 4. Fraction of particles hitting vessel walls as a function of particle radius. Cases 1 and 2 defined in Fig. 2. Solid lines and symbols represent the loss for steady state conditions as determined from Equation (9); dashed lines and hollow symbols represent condition when the fluid spins up after being initially at rest. Fall velocities are characteristic of phytoplankton.

particle has a trajectory which intersects the cylinder wall. If particles are initially uniformly distributed in a tube with the fluid at steady state, then the fraction f_{ss} of particles which do not hit the walls is proportional to the area of their circle

$$f_{ss} = \frac{(a - x_b)^2}{a^2} = \left(1 - \frac{w_s}{a\omega}\right)^2. \quad (9)$$

The fraction that hits the wall g_{ss} equals $1 - f_{ss}$. It increases with the sinking rate and, hence, the size of the falling particle (Fig. 4).

Fluid initially at rest

Particle trajectories when the fluid is initially at rest are much more complicated (Fig. 5). Particles in the interior can fall substantial distances before they become entrained in the fluid rotation. As a result, the fraction of particles which hit the container wall is greater than g_{ss} when g_{ss} is large fraction of all the particles (Fig. 4). This movement of particles causes non-uniform concentrations of particles, particularly when g_{ss} is large.

DISCUSSION

The goal of developing a laboratory coagulation reactor is to design a simple system in which the particles collide under simple, well understood conditions. It helps if only one of the coagulation mechanisms dominates. The rotating cylinder suffers from several flaws.

In the process of starting up, the shears can be substantial and can last for significant periods. For example, the larger reactor used as an example would have shears greater

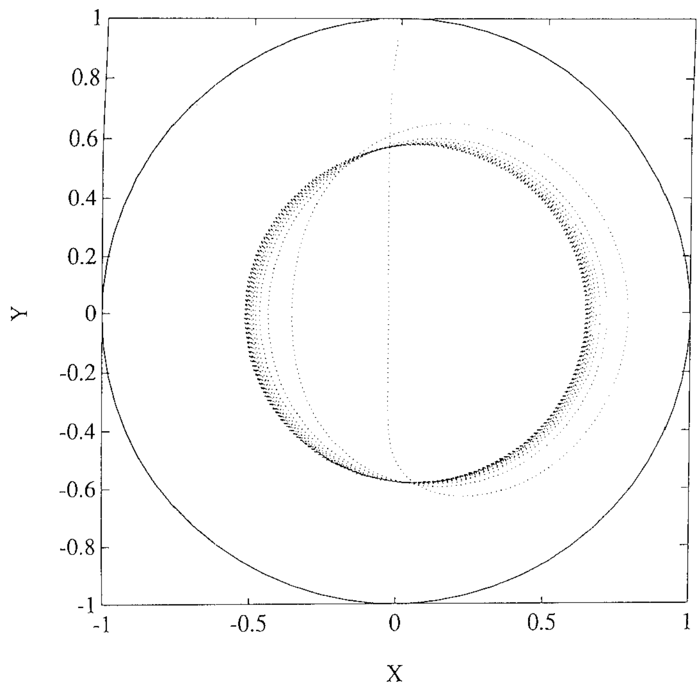

Fig. 5. Sample particle trajectory during spin up for Case 2 when the particle is 300 μm radius, with $w_s = 600\,\mu\text{m s}^{-1}$. This particle does not hit the cylinder wall but still moves substantially from its initial position.

than the high shear rate of 1 s^{-1} for more than 8 min. Shears would be greater than 0.1 s^{-1} for considerably longer. These high shear rates can be reduced by using a smaller cylinder and rotating it more slowly. However, even the smaller containers have shear rates that are much larger than the 0.1–0.01 s^{-1} that is characteristic of oceanic waters (e.g. Soloviev *et al.*, 1988).

Small containers rotating at slow speeds do not have shear rates that are as high nor do they last as long. However, their slower rotational velocities exclude larger fractions of particles from achieving stable orbits without hitting the sides of their containers (Fig. 5, 6). Hitting the container sides can change the probability of particle-particle collision, as a particle can hit the particles that have been concentrated there. It will also cause a greater concentration of particles in the outer edge of the stable zone (Fig. 6).

The trajectory and resulting particle distribution shown in Figs 5 and 6 is for a particle larger than the typical phytoplankter (300 μm). However, this particular fall velocity does provide a dramatic illustration of the consequences of the redistribution of particles associated with the rotating cylinder system. Aggregation experiments focus on the development of particles this large and larger.

Particles in natural waters occur over a range of sizes usually characterized by a size spectrum. Each group of particles would have its own stable region and concentration distribution. The interaction rates of all the particles would depend on these distributions. Calculating collision rates in such a container would be extremely complex. Not only do

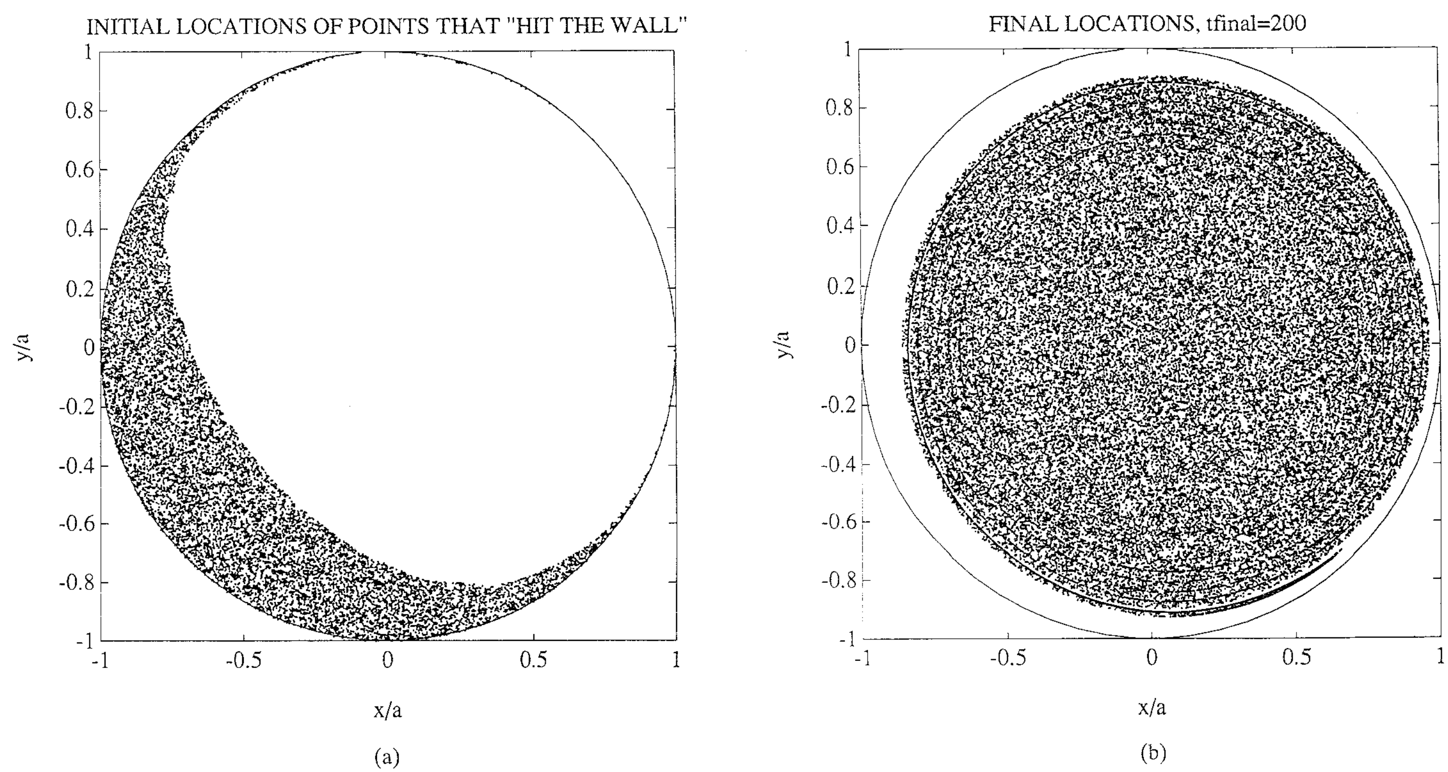

Fig. 6. Distributions from 500,000 particles initially distributed randomly throughout the cylinder before spin up. (A) initial location of particles which hit the cylinder; (B) location of all particles after the initial transients have dissipated. Notice that there is a spiral of particles in the outer part of the final mass of particles that is formed by the particles that hit the cylinder wall. Parameters as in Fig. 5.

the different particles have different stable regions, an aggregating particle would have to move from one region to another as it grows.

The exact effect on particle distributions and coagulation rates are difficult to give because they will depend on the incubation conditions, including initial particle concentration and incubation length. The relative amount of aggregation occurring during the high shear start up phase will depend on the period of the incubation, as well as on the initial particle concentration. Longer periods will allow differential sedimentaion to become relatively more important. However, it is the variability of the effect that adds uncertainty to the interpretation of the results.

Tooby *et al.* (1977) analyzed particle trajectories, accounting for centrifugal effects associated with the particles going in circles, as well as interactions between the walls and the particle. They found that the particles could spiral slowly inward or outward but did not discuss the rates at which this happens. The inclusion of these higher order effects further complicate understanding what happens during coagulation in such a system.

Acknowledgements—T. Caillouet assisted with the calculations. B. Logan encouraged the analysis. This work was supported by Office of Naval Research Contract N0001487-K0005 and U.S. Department of Energy Grant DE-FG05-85-ER60341.

REFERENCES

Berg H. C. (1983) *Random walks in biology*. Princeton University Press, Princeton, New Jersey, 142 pp.

Camp T. R. and P. C. Stein (1943) Velocity gradients and internal work in fluid motion. *Journal of the Boston Society of Civil Engineers*, **30**, 219–237.

Carslaw H. S. and J. C. Jaeger (1959) *Conduction of heat in solids*, 2nd edn. Clarendon Press, Oxford, 510 pp.

Happel J. and H. Brenner (1973) *Low Reynolds Number hydrodynamics*, 2nd edn. Martinus Nijhoff, New York, 553 pp.

Jackson G. A. (1989) Simulation of bacterial attraction and adhesion to falling particles in an aquatic environment. *Linmology and Oceanography*, **34**, 514–530.

Jackson, G. A. and S. E. Lochmann (1992) Effect of coagulation on nutrient and light limitation of an algal bloom. *Limnology and Oceanography*, **37**, 77–89.

McCave I. N. (1984) Size spectra and aggregation of suspended particles in the deep ocean. *Deep-Sea Research*, **31**, 329–352.

Shanks A. L. and E. W. Edmondson (1989) Laboratory-made artificial marine snow: a biological model of the real thing. *Marine Biology*, **101**, 463–470.

Smayda T. R. (1970) The suspension and sinking of phytoplankton in the sea. *Oceanography and Marine Biology, Annual Review*, **8**, 353–414.

Soloviev A.V., N. V. Vershinsky and V. A. Bezverchnii (1988) Small-scale turbulence measurements in the thin surface layer of the ocean. *Deep-Sea Research*, **35**, 1859–1874.

Tooby P. F., G. L. Wick and J. D. Isaacs (1977) The motion of a small sphere in a rotating velocity field: a possible mechanism for suspending particles in turbulence. *Journal of Geophysical Research*, **82**, 2096–2100.